Terahertz and FTIR spectroscopy of 'Bisphenol A'

Ramzan Ullah [a], Han Li [b], YiMing Zhu [a,*]

[a] Shanghai Key Lab of Modern Optical System, Engineering Research Center of Optical Instrument and System, Ministry of Education, University of Shanghai for Science and Technology, No. 516 JunGong Rd., Shanghai 200093, China
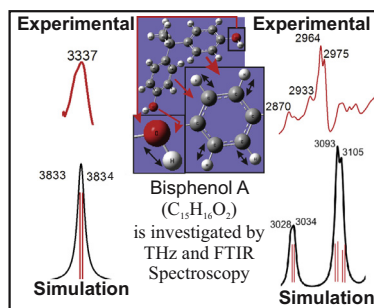[b] Shanghai First Rehabilitation Hospital, Shanghai 200090, China

HIGHLIGHTS

- 'Bisphenol A' is investigated at THz (0.2–2 THz) and FTIR (400–4000 cm^{-1}).
- Refractive index (0.2–2 THz) is almost constant with an average value of 1.34.
- An absorption peak at 1.69 THz is found and assigned by DFT.
- FTIR (400–4000 cm^{-1}) spectra agree with DFT except C–H and O–H stretching freq.
- MOLVIB is used to rescale the simulated frequencies to match experimental values.

GRAPHICAL ABSTRACT

The C–H and O–H stretching regions and corresponding simulated results.

ABSTRACT

Time domain terahertz (0.2–2 THz) and FTIR (400–4000 cm^{-1}) spectra of 'Bisphenol A' are presented. An average refractive index of 1.34 from 0.2 to 2 THz and an absorption peak at 1.69 THz that is considered as the twisting of aromatic rings with hydroxyl groups along the shared carbon atom are found. The simulated results by using density functional theory (DFT) with B3LYP 6-311++G (3df, 3pd), B3LYP 6-31G (3df 3pd) and B3LYP 3-21G after anharmonic corrections are well agreed with the experimental results. Furthermore, Pulay's Method is adopted to overcome the incapability of DFT in describing C–H and O–H stretching interactions to match with experimental values.

© 2013 Elsevier B.V. All rights reserved.

1. Introduction

A strip between the microwave and infrared region of electromagnetic spectrum is named as terahertz band spanning from 0.1 to 10 THz [1]. Terahertz time domain spectroscopy (THz-TDS) has been applied tremendously in the fields of materials characterization [2–6]. Low frequency vibrations, refractive index and dielectric character of molecule can be obtained from the THz-TDS technique that could provide useful information about molecular structure and properties [7,8].

'Bisphenol A' (BPA) is a widespread endocrine-disrupting chemical used in the manufacturing of polycarbonate plastics and epoxy resins such as food packaging industries. As a hormonally active chemical BPA has been received increasing attention due to its high potential risks for human exposure. The material is correlated to a set of adverse health effects and may be a possible neurotoxin, genotoxic, endocrine disruptor and carcinogen according to World Health Organization [9–11]. 'Bisphenol A' has been studied by FTIR spectroscopy but it focuses on the intermolecular hydrogen bond

between poly-(3-hydroxybutyrate co-3-hydroxyvalerate) (PHBV) and BPA blends [12]. It is essential to comprehensively investigate the structure of BPA (see Fig. 1) which would be useful for detection and behavior of this molecule. In this study, THz-TDS and Fourier Transform Infrared Spectroscopy (FTIR) are used to study the low and high frequency vibrations of the BPA that may help to understand the molecular structure and dynamics. Density functional theory (DFT) is adopted to analyze the spectra from experiments and they agree well with each other except C–H and O–H stretching zones.

2. Experimental setup

An ultrafast Fiber Laser System (Near-Infrared System FemtoFiber Pro NIR from TOPTICA Photonics) is used to generate femtosecond laser pulses [13]. The THz setup is THz Time-Domain Spectroscopy System [14] which is similar with the system used in our previous work [15–17]. The THz emitter and detector is low temperature grown Gallium Arsenide (LTG-GaAs) photoconductive switch. Signal to noise ratio is more than 10^5: 1 at 0.4 THz. The whole setup is in a box and purged with dry air to eliminate the relative humidity and temperature is maintained around 23 °C.

3. Sample preparation

'Bisphenol A' CAS No, [80-05-7] is ground to very fine powder and pressed homogeneously between two plates of polystyrene. Refractive index and absorption coefficient of polystyrene is determined first with air as reference. Eq. (1) is used for refractive index and Eq. (2) for absorption coefficient by setting n_p = 1. A nearly constant refractive index of 1.58 and nearly zero absorption coefficient of polystyrene (0.2–2 THz) is calculated which is consistent with the literature [18]. Thickness is determined by a digital micrometer capable to measure the thickness up to 0.001 mm precision. Reference cell for 'Bisphenol A" is prepared by joining two polystyrene plates without any space in between.

4. Data analysis

Terahertz refractive index 'n_{sample}' and absorption coefficient α_{sample} of 'Bisphenol A' is calculated by Eqs. (1) and (2) respectively.

$$n_{sample} = 1 + (\varphi_S - \varphi_R)\frac{c}{\omega d} \tag{1}$$

$$\alpha_{sample} = -\frac{2}{d} \ln \left[\frac{A_{sample}}{A_{reference}} \times \frac{(n_P + n_{sample})^2}{4n_P n_{sample}} \right] \tag{2}$$

Sample amplitude 'A_{sample}', Reference amplitude '$A_{reference}$', sample phase 'φ_S' and reference phase 'φ_R; are put from experimental data after performing FFT on time domain traces in above formulae. 'ω' is angular frequency, 'c' is speed of light, 'd' is sample thickness and 'n_p' is the refractive index of polystyrene whose value was taken as 1.58. Error bars are showing 95% confidence interval calculated from the standard deviation of the mean. Error bars are almost constant for the refractive index and minimum for absorption coefficient in the range 0.2–1.08 THz. Error bars are large in the high frequency range for absorption coefficient because of low signal to noise ratio caused by week input signal and large absorption in high frequency region. Time domain reference and sample pulses along with their FFTs are shown in Fig. 2. The signal is cutoff before the first echoes before performing FFT.

5. DFT analysis

DFT calculations are carried out in Gaussian 09 package [19] optimized to minimum and Ground State method B3LYP along with 6-311G basis set [20] together with (3df, 3pd) and ++ diffuse functions [21]. Three different configurations (DFT) B3LYP 6-311++G (3df, 3pd), (DFT) B3LYP 6-31G (3df 3pd) and (DFT) B3LYP 3-21G are used. The calculated vibrational spectra are compared with experimental results on the basis of which absorption peaks are assigned to relevant molecular vibrations.

6. Results and discussion

As shown in Fig. 3, refractive index of 'Bisphenol A' is almost constant from 0.2 to 2 THz with an average value of 1.34. Absorption coefficient has an average value of 16.18 cm^{-1} and an absorption peak from experiment at 1.69 THz was observed which is associated to the twisting of its aromatic rings with hydroxyl groups along the shared carbon atom (see Supplementary material) revealed by DFT B3LYP 6-311G ++(3df 3pd) calculations at 1.6411 THz which agrees well with experimental value after scaling with scale factor 1.0100 for low frequency vibrations calculated by Andersson and Uvdal [22] to correct anharmonicity generally
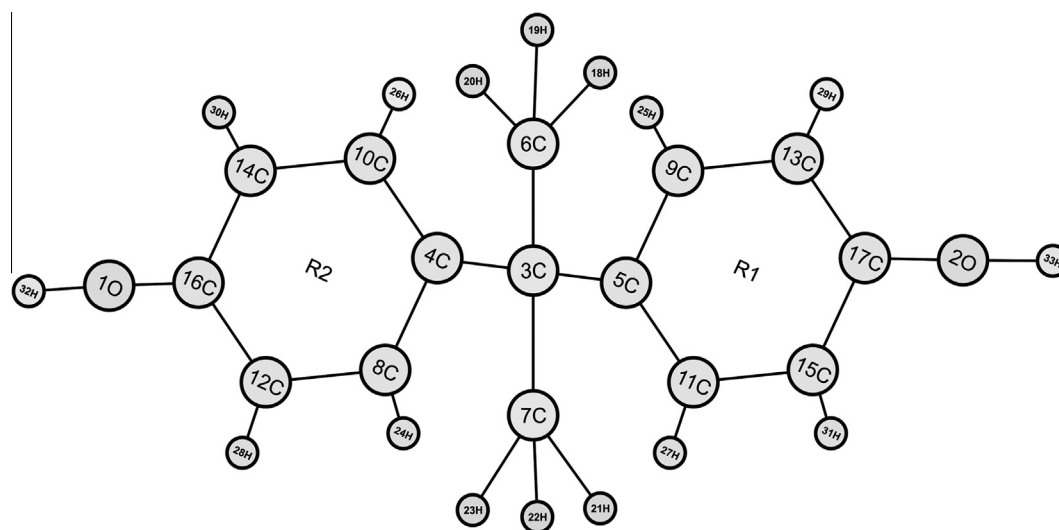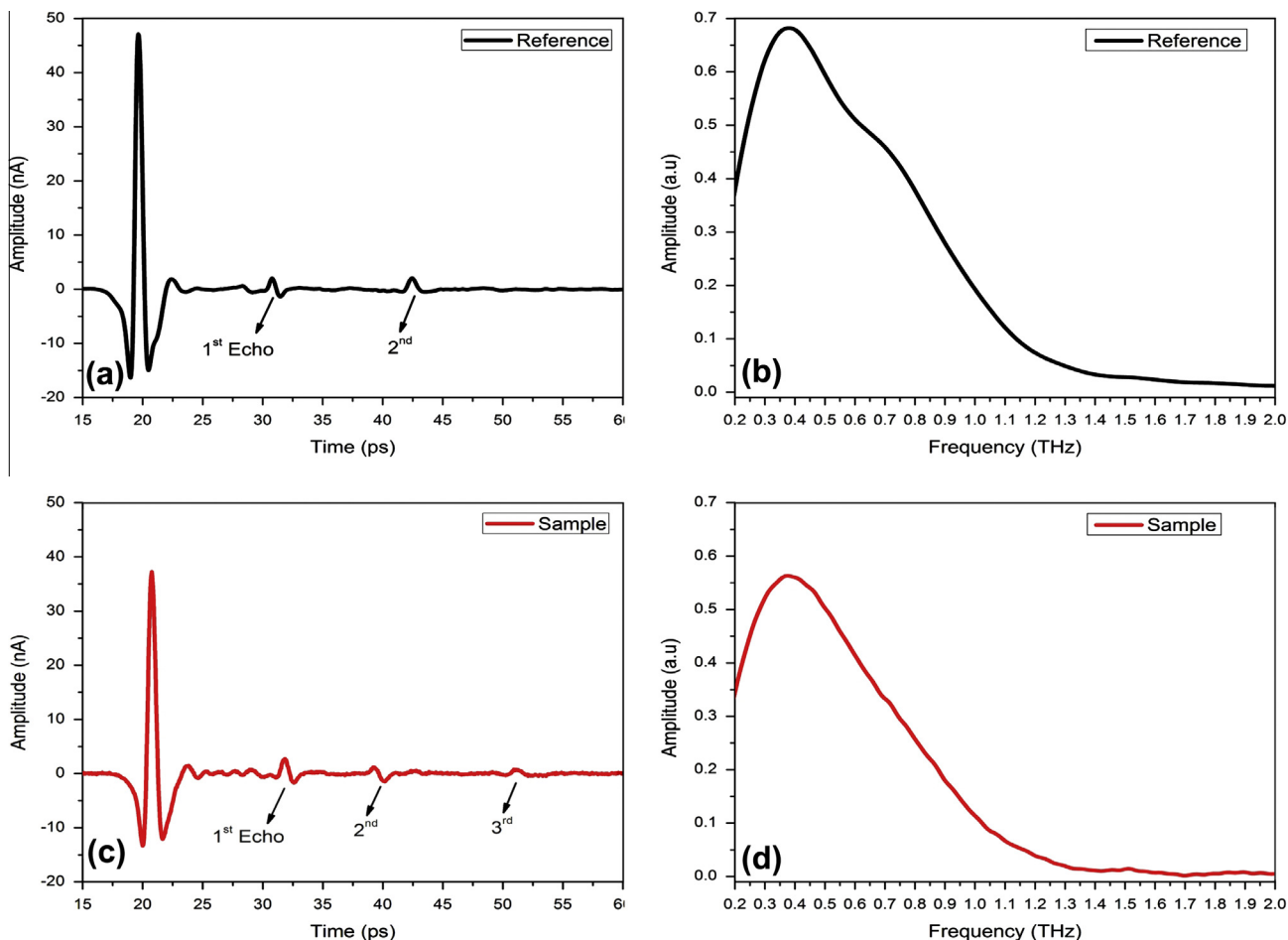

Fig. 1. Bisphenol A.

Fig. 2. (a) Time domain trace of reference which is two PS plates together without any space in between. (b) FFT of reference. (c) Time domain trace of Sample which is 'Bisphenol A' pressed between two PS plates. (d) FFT of sample.

induced in DFT calculations. B3LYP 6-31G(3df 3pd) and B3LYP 3-21G methods also agree at this frequency with a value of 1.63 THz but deviates significantly for other two vibrational modes in this frequency range as shown in Table 1. However, two other predicted absorption peaks by DFT are absent in the experimental absorption spectrum. As 'Bisphenol A' is a slightly polarized organic molecule, an abrupt decline of refractive index can be seen at the frequency of absorption peak [23]. Hence BPA is detectable by Terahertz spectroscopy.

Furthermore, FTIR (400 – 4000 cm^{-1}) spectrum is shown along with DFT values in the Fig. 4. It is clear that DFT and experimental values are reasonably in good agreement in the range 400–1700 cm^{-1} after scaling with the scale factor of 0.9679 for vibrational frequencies calculated by Andersson and Uvdal [22]. However, DFT values are deviating over a large extent from experimental values in the C–H and O–H stretching zones showing the limitation of DFT in describing such interactions. Although B3LYP 3-21G is giving the better match to experimental values for O–H stretching frequencies but difference is still too high. Usual method of least squares fit is used to find a common scaling factor [24] by minimizing the difference,

$$D = \sum_{i}^{all} (\kappa w_i^{theoretical} - w_i^{experimental})^2 \qquad (3)$$

where 'κ' is the required scale factor and "$w_i^{theoretical}$" and" $w_i^{experimental}$" are the ith theoretical harmonic and experimental frequencies (cm^{-1}). In the minimization process, high frequency vibra-
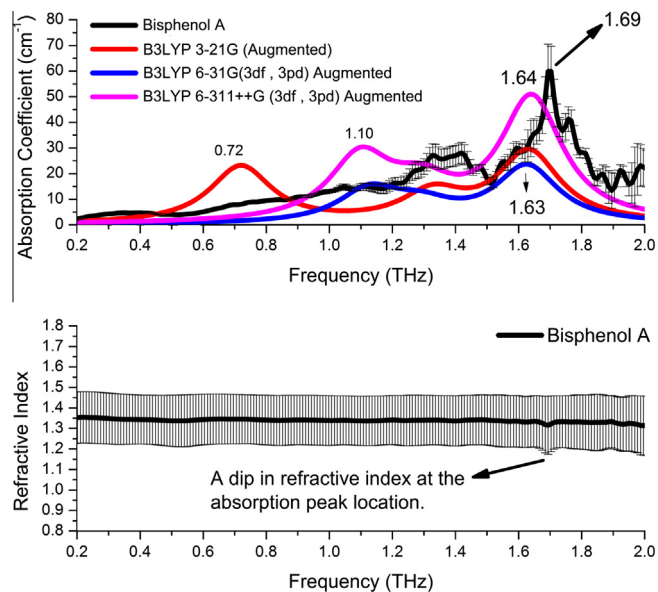

Fig. 3. Refractive index and absorption coefficient of 'Bisphenol A' along with DFT results with 3 different configurations (colors online). Numerical values have been fixed to two decimal places. See Table 1 for detail.

tions dominate the RMS (Root Mean Squares) and ultimately the scale factor. Low frequencies contribute more to thermodynamic

Table 1
List of vibrational modes of 'Bisphenol A' predicted by three DFT calculations with different configurations in the range (0.2–2 THz).

Vibrational modes	B3LYP 6-311G ++(3df 3pd) (THz)	B3LYP 6-31G(3df 3pd) (THz)	B3LYP 3-21G (THz)
1	1.0977	1.1275	0.7194
2	1.2939	1.2949	1.3290
3	1.6411	1.6267	1.6324
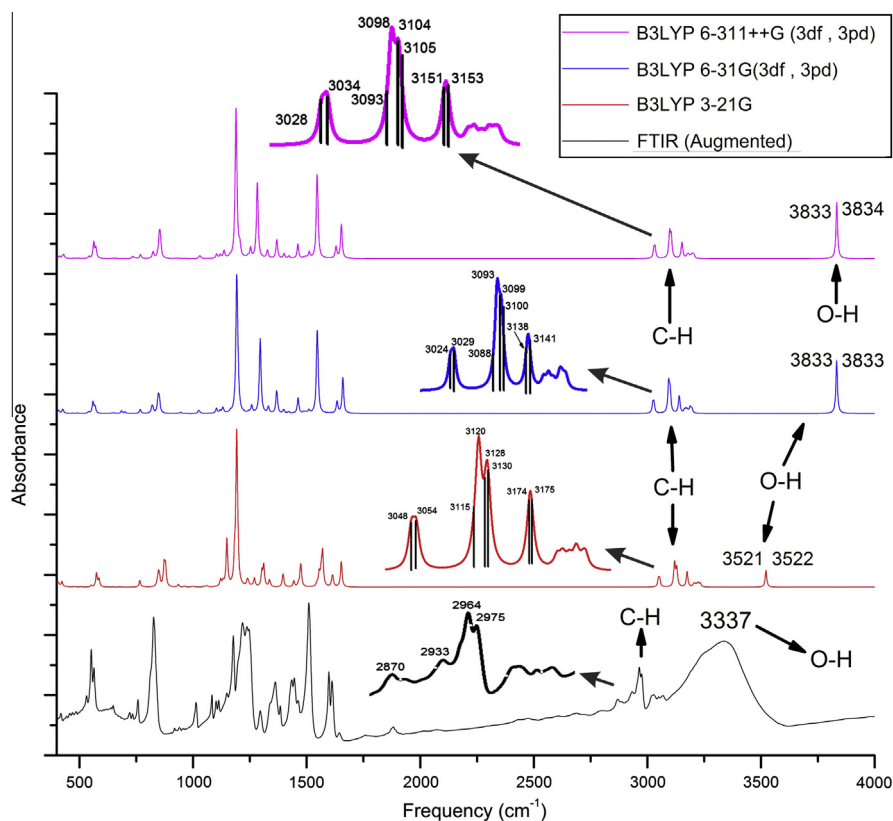
Fig. 4. FTIR and DFT spectra with 3 different configurations of 'Bisphenol A'. Numerical values have been converted to whole numbers. See Table 2 for detail.

processes than high frequencies, [25] so a least square fit of inverse vibration frequencies is obtained to determine the scale factor for low frequencies by minimizing the sum in Eq. (4).

$$D_{low} = \sum_{i}^{all} \left(\frac{1}{\kappa w_i^{theoretical}} - \frac{1}{w_i^{experimental}} \right)^2 \qquad (4)$$

The method given in Eq. (3) determines the scale factor very well for the frequencies given in the range 400–1700 cm^{-1} of Fig. 4. However, because the deviations in region C–H and O–H are not systematic, it is not effective for those absorption peaks in those frequency regions. If we take DFT B3LYP 6-311G ++(3df 3pd) frequencies only from region C–H and O–H as given in Table 2 unscaled, it does not give the best fit and gives a slope (scale factor) of 0.5426 which makes all the frequencies about half of their original values showing the limitation of this method. This situation suggests that multiple scale factors must be determined based on different interactions between atoms.

Pulay et al. [26] introduced a formula to calculate scale factors transferable between similar molecules subject to the condition that suitable internal coordinates are chosen. If '$F_{x,y}$' represent un-scaled force constants, then

$$F'_{x,y} = \sqrt{\kappa_x \kappa_y} F_{x,y}, \qquad (5)$$

where '$F'_{x,y}$' are scaled force constants and κ_x, κ_y are the scale factors. This method requires choosing suitable internal coordinates. Internal coordinates of 'Bisphenol A' can be found in Supplementary material.

MOLVIB program [27,28] was used, which uses the Pulay's method to rescale the calculated frequencies [29]. Internal coordinates of 'Bisphenol A' (given in Supplementary material) are fed to the MOLVIB by fixing all other scale factors except C–H and O–H factors and as a result we can see in the Table 2, those frequency modes along with the assigned DFT values (both scaled and unscaled) and potential energy distributions (PEDs) analysis which is also done by MOLVIB. From the analysis, it is revealed that the suitable scale factors (force constants) for C–H and O–H stretching for B3LYP 6-31G (3df 3pd) are 0.91103 and 0.75834, for B3LYP 6-311G ++ (3df 3pd) are 0.90814 and 0.75800 and for B3LYP 3-21G are 0.89549 and 0.89686 respectively. O–H stretching frequencies are now matching at marvelous accuracy while those for C–H stretching are also in good agreement as given in Table 2.

7. Conclusion

We have determined refractive index with an average value of 1.34 and absorption coefficient with an average value of

Table 2
A comparison of FTIR observed frequencies in the OH and CH stretching zones along with DFT results with 3 different configurations both unscaled and scaled with MOLVIB together with PED (%).

FTIR Observed (cm^{-1})	B3LYP 6-311G ++(3df 3pd) (cm^{-1}) (%)		B3LYP 6-31G(3df 3pd) (cm^{-1}) (%)		B3LYP 3-21G (cm^{-1}) (%)	
2870	(3028.4)$_{unscaled}$ (2887.5)$_{scaled}$	CH3a (59), CH3b (41)	(3023.6)$_{unscaled}$ (2887.4)$_{scaled}$	CH3a (59), CH3b (41)	(3048.5)$_{unscaled}$ (2886.5)$_{scaled}$	CH3a (71), CH3b (29)
2870[a]	(3033.6)$_{unscaled}$ (2892.8)$_{scaled}$	CH3b (59), CH3a (41)	(3028.7)$_{unscaled}$ (2892.7)$_{scaled}$	CH3b (59), CH3a (41)	(3053.8)$_{unscaled}$ (2892.0)$_{scaled}$	CH3b (71), CH3a (29)
2933	(3093.1)$_{unscaled}$ (2944.9)$_{scaled}$	CH3a (57), CH3b (42)	(3088.2)$_{unscaled}$ (2945.1)$_{scaled}$	CH3a (55), CH3b (44)	(3115.2)$_{unscaled}$ (2944.8)$_{scaled}$	CH3a (63), CH3b (36)
2964	(3097.9)$_{unscaled}$ (2950.0)$_{scaled}$	CH3b (56), CH3a (44)	(3093.4)$_{unscaled}$ (2950.6)$_{scaled}$	CH3a (46), CH3b (53)	(3119.8)$_{unscaled}$ (2949.2)$_{scaled}$	CH3b (60), CH3a (40)
2975	(3104.1)$_{unscaled}$ (2955.8)$_{scaled}$	CH3a (77), CH3b (22)	(3098.6)$_{unscaled}$ (2955.1)$_{scaled}$	CH3a (73), CH3b (26)	(3128.3)$_{unscaled}$ (2956.3)$_{scaled}$	CH3a (67), CH3b (32)
2975[a]	(3105.4)$_{unscaled}$ (2957.0)$_{scaled}$	CH3b (79), CH3a (20)	(3100.4)$_{unscaled}$ (2957.2)$_{scaled}$	CH3b (75), CH3a (24)	(3130.0)$_{unscaled}$ (2959.3)$_{scaled}$	CH3b (71), CH3a (29)
3337	(3833.1)$_{unscaled}$ (3336.6)$_{scaled}$	OH (100)	(3832.8)$_{unscaled}$ (3336.7)$_{scaled}$	OH (100)	(3521.4)$_{unscaled}$ (3335.6)$_{scaled}$	OH (100)
3337[a]	(3834)$_{unscaled}$ (3337.4)$_{scaled}$	OH (100)	(3833.3)$_{unscaled}$ (3337.3)$_{scaled}$	OH (100)	(3522.1)$_{unscaled}$ (3338.4)$_{scaled}$	OH (100)

[a] Multiple assignment.

16.18 cm^{-1} of 'Bisphenol A' in the range (0.2–2 THz). An absorption peak was found at 1.69 THz which is associated to the twisting of aromatic rings with hydroxyl groups along the shared carbon atom revealed by DFT calculations. FTIR (400–4000 cm^{-1}) spectrum conforms well to DFT calculated frequencies except C–H and O–H stretching regions. We have also used Pulay's method employed by MOLVIB to overcome the flaw of DFT in describing the stretching interaction of Hydrogen with Carbon and Oxygen.

Appendix A. Supplementary material

Supplementary data associated with this article can be found, in the online version, at http://dx.doi.org/10.1016/j.molstruc.2013.11.055.

References

[1] Yun-Shik Lee, Principles of Terahertz Science and Technology, Springer Science + Business Media, LLC, 2009. Chapter 1.
[2] D. Grischkowsky, Soren Keiding, Martin van Exter, Ch. Fattinger, J. Opt. Soc. Am. B 7 (10) (1990).
[3] R. Piesiewicz, C. Jansen, S. Wietzke, D. Mittleman, M. Koch, T. Kürner, Properties of building and plastic materials in the THz range, Int. J. Infrared Milli Waves, Springer Science + Business Media, LLC, 2007. doi: 10.1007/s10762-007-9217-9.
[4] A. Katsounaros et al., Carbon (2011), http://dx.doi.org/10.1016/j.carbon.2011.09.056.
[5] B. Yu, F. Zeng, Y. Yang, Q. Xing, A. Chechin, X. Xin*, I. Zeylikovich, R.R. Alfano, Biophys. J. 86 (2004) 1649–1654.
[6] Joseph S. Melinger, S. Sree Harsha, N. Laman, D. Grischkowsky, Opt. Exp. 18 (26) (2010) 27238.
[7] Cecilie Ronne, Soren Rud Keiding, J. Mol. Liquids (2002), 101/1-3 199–218.
[8] Jianming Dai, Jiangquan Zhang, Weili Zhang, D. Grischkowsky, J. Opt. Soc. Am. B 21 (7) (2004).
[9] <http://www.who.int/foodsafety/chem/chemicals/bisphenol/en/index.html> (accessed 07.01.13, 07:18AM CST).
[10] <http://whqlibdoc.who.int/publications/2011/97892141564274_eng.pdf> (accessed 07.01.13, 07:18AM CST).
[11] Guy Riddihough, Science 340 (6140) (2013) 1500, http://dx.doi.org/10.1126/science.340.6140.1500-a.
[12] Bin Fei, Cheng Chen, Hang Wu, Shuwen Peng, Xiuyan Wang, Lisong Dong, Eur. Polym. J. 39 (2003) 1939–1946.
[13] <http://www.toptica.com/products/ultrafast_fiber_lasers/femtofiber_pro/femtofiber_pro_nir.html> (accessed 07.01.13, 07:18AM CST).
[14] <http://www.ekspla.com/product/t-spec-series-real-time-terahertz-spectrometer> (accessed 26.01.13, 12:54AM CST).
[15] S.Q. Du, H. Li, L. Xie, L. Chen, Y. Peng, Y.M. Zhu, H. Li, P. Dong, J.T. Wang, Appl. Phys. Lett. 100 (2012) 143702, http://dx.doi.org/10.1063/1.3700808.
[16] Lin Chen, Yiming Zhu, Xiaofei Zang, Bin Cai, Zhou Li, Le Xie, Songlin Zhuang, Light: Sci. Appl. (2013) 2, e60, doi: 10.1038/lsa.2013.16. (published online 29 March 2013).
[17] Lin Chen, Chunmei Gao, Jiaming Xu, Xiaofei Zang, Bin Cai, Yiming Zhu1, Opt. Lett. 38 (9) (2013).
[18] Paul D. Cunningham, Nestor N. Valdes, Felipe A. Vallejo, L. Michael Hayden, Brent Polishak, Xing-Hua Zhou, Jingdong Luo, Alex K.-Y. Jen, Jarrod C. Williams, Robert J. Twieg, J. Appl. Phys. 109 (2011) 043505.
[19] Gaussian 09, Revision A.01, M.J. Frisch, G.W. Trucks, H.B. Schlegel, G.E. Scuseria, M.A. Robb, J.R. Cheeseman, G. Scalmani, V. Barone, B. Mennucci, G.A. Petersson, H. Nakatsuji, M. Caricato, X. Li, H.P. Hratchian, A.F. Izmaylov, J. Bloino, G. Zheng, J.L. Sonnenberg, M. Hada, M. Ehara, K. Toyota, R. Fukuda, J. Hasegawa, M. Ishida, T. Nakajima, Y. Honda, O. Kitao, H. Nakai, T. Vreven, J. A. Montgomery, Jr., J.E. Peralta, F. Ogliaro, M. Bearpark, J.J. Heyd, E. Brothers, K.N. Kudin, V.N. Staroverov, R. Kobayashi, J. Normand, K. Raghavachari, A. Rendell, J.C. Burant, S.S. Iyengar, J. Tomasi, M. Cossi, N. Rega, J. M. Millam, M. Klene, J.E. Knox, J.B. Cross, V. Bakken, C. Adamo, J. Jaramillo, R. Gomperts, R.E. Stratmann, O. Yazyev, A.J. Austin, R. Cammi, C. Pomelli, J.W.Ochterski, R.L. Martin, K. Morokuma, V.G. Zakrzewski, G.A. Voth, P. Salvador, J.J. Dannenberg, S. Dapprich, A.D. Daniels, O. Farkas, J.B. Foresman, J.V. Ortiz, J. Cioslowski, D.J. Fox, Gaussian Inc, Wallingford CT, 2009.
[20] V. Rassolov, J.A. Pople, M. Ratner, P.C. Redfern, L.A. Curtiss, J. Comp Chem. (2001), 22(9) 976–984.
[21] T. Clark, J. Chandrasekhar, G.W. Spitznagel, P.v.R. Schleyer, J. Comp. Chem. 4 (1983) 294–301.
[22] M.P. Andersson, P. Uvdal, J. Phys. Chem. A 109 (2005) 2937–2941.
[23] Liangliang Zhang et al., Appl. Phys. Lett. 92 (2008) 091117, http://dx.doi.org/10.1063/1.2891082.
[24] Yuthana Tantirungrotechai, Ketthip Phanasant, Supacharee Roddecha, Panida Surawatanawong, Vallaya Sutthikhum, Jumras Limtrakul, J. Mol. Struct.: THEOCHEM 760 (2006) 189–192.
[25] Anthony.P. Scott, Leo. Radom, J. Phys. Chem. 100 (1996) 16502–16513.
[26] P. Pulay, G. Gorarasi, G. Pongor, J.E. Boggs, A. Vargha, J. Am. chem. Soc. 105 (1983) 7037.
[27] T. Sundius, J. Mol. Struct. 218 (1990) 321.
[28] T. Sundius, J. Mol. Spectrosc. 82 (1980) 138.
[29] T. Sundius, Vib. Spectrosc. 29 (2002) 89–95.